DRUG DELIVERY
2022, VOL. 29, NO. 1, 2705–2712
https://doi.org/10.1080/10717544.2022.2110998

Taylor & Francis
Taylor & Francis Group

RESEARCH ARTICLE

OPEN ACCESS Check for updates

Prostate-specific membrane antigen targeted, glutathione-sensitive nanoparticles loaded with docetaxel and enzalutamide for the delivery to prostate cancer

Yang Chen[a], Zhenyu Xu[b], Tingxun Lu[b], Jia Luo[c] and Hua Xue[d]

[a]Affiliated Hospital of Jiangnan University, Wuxi214000, Jiangsu Province, China; [b]Department of Oncology, Affiliated Hospital of Jiangnan University, Wuxi214000, Jiangsu Province, China; [c]Department of Pharmacy, Affiliated Hospital of Nantong University, Nantong226000, Jiangsu Province, China; [d]Department of Pharmacy, Wuxi Mental Health Center, Wuxi214000, Jiangsu Province, China

ABSTRACT

Prostate cancer (PCa) is the most common malignant tumor in men. Chemotherapy with docetaxel (DTX) and novel hormonal agents such as enzalutamide (EZL) and abiraterone are the preferred first-line therapeutic regimens. Prostate-specific membrane antigen (PSMA) is overexpressed on the surface of PCa cells. This study aimed to prepare a PSMA targeted (Glutamate-Urea-Lysine, GUL ligand modified), glutathione (GSH)-sensitive (Cystamine, SS), DTX and EZL co-loaded nanoparticles (GUL-SS DTX/EZL-NPs) to treat PCa. Polyethylene glycol (PEG) was conjugated with oleic acid (OA) using a GSH-sensitive ligand: cystamine (PEG-SS-OA). GUL was covalently coupled to PEG-SS-OA to achieve GUL-PEG-SS-OA. GUL-PEG-SS-OA was used to prepare GUL-SS DTX/EZL-NPs. To evaluate the *in vitro* and *in vivo* efficiency of the system, human prostate cancer cell lines and PCa cells bearing mice were applied. Single drug-loaded nanoparticle and free drugs systems were utilized for the comparison of the anticancer ability. GUL-SS DTX/EZL-NPs showed a size of 143.7 ± 4.1 nm, with a PDI of 0.162 ± 0.037 and a zeta potential of +29.1 ± 2.4 mV. GUL-SS DTX/EZL-NPs showed high cancer cell uptake of about 70%, as well as higher cell growth inhibition efficiency (a maximum 79% of cells were inhibited after treatment) than single drug-loaded NPs and free drugs. GUL-SS DTX/EZL-NPs showed the most prominent tumor inhibition ability and less systemic toxicity. The novel GUL-SS DTX/EZL-NPs could be used as a promising system for PCa therapy.

ARTICLE HISTORY
Received 14 July 2022
Revised 1 August 2022
Accepted 1 August 2022

KEYWORDS
Prostate cancer; prostate-specific membrane antigen; glutathione responsive; nanoparticles; docetaxel; enzalutamide

Introduction

Prostate cancer (PCa) is the most common malignant tumor in men, the second leading cause of cancer death after lung cancer, and the most common tumor in over one hundred countries (Jemal et al., 2011; Li et al., 2012). Based on the National Comprehensive Cancer Network (NCCN) guidelines for PCa, docetaxel (DTX) is standard chemotherapy and the only treatment that has been shown to improve overall survival for advanced PCa (Berthold et al., 2008; Yan et al., 2016).

Chemotherapy with DTX and novel hormonal agents such as enzalutamide and abiraterone are the preferred first-line therapeutic regimens based on different progressions of Castration-Resistant Prostate Cancer (CRPC) (Scher et al., 2012; Kellokumpu-Lehtinen et al., 2013; Fizazi et al., 2014). Specifically DTX with prednisone is the traditional mainstay of treatment for symptomatic CRPC (Tannock et al., 2004; Berthold et al., 2008). Enzalutamide (EZL) with prednisone, the newer therapy, has been recommended by the NCCN guidelines as first-line therapy for patients with asymptomatic or minimally symptomatic metastatic CRPC (Scher et al., 2012; "A safety and efficacy study of oral MDV3100 in chemotherapy-naïve patients with progressive metastatic prostate cancer (PREVAIL) (NCT01212991)", 2014). Meanwhile, researches have proven that concomitant enzalutamide and taxanes were synergistic, and prior enzalutamide reduced DTX cytotoxicity in Vertebral Cancer of the Prostate (VCaP) cells (Marín-Aguilera et al., 2019). Therefore, it is anticipated that combination therapy of DTX and enzalutamide for CRPC would bring a new future. It is an urgent need for engineering a drug delivery system with different pharmacokinetic action for both drugs.

Nanocarrier-based drug delivery systems are currently developed to improve the survival and clinical outcome of the drugs (Zhang et al., 2017). The nanocarriers may introduce controlled drug release ability and improving antitumor activity by responding to environmental stimuli (such as pH or reduction) in the tumor microenvironment (Wang et al., 2019). For example, Kim et al. used a gelatin–oleic acid (OA) sodium salt conjugate as a novel solubilizing adjuvant to prepare nanocarriers for delivering poorly water-soluble drugs (Kim et al., 2020). Phan et al. developed a Fucoidan–OA conjugate for the co-delivery of curcumin and paclitaxel (Phan et al.,

CONTACT Yang Chen chenyjnu@outlook.com Department of Pharmacy, Affiliated Hospital of Jiangnan University, Wuxi 214000, Jiangsu Province, China

2016). One of the important characteristics of PCa is significantly higher (fourfold higher) glutathione (GSH) level (Argenziano et al., 2018; Xu et al., 2018). Besides, tumor cells contain higher concentration of GSH than normal cells (Xu et al., 2015). So GSH has emerged as a popular biodegradable polymer and GSH-sensitive linkage (disulfide) has been extensively evaluated in GSH-sensitive drug delivery systems for cancer therapy (Jabir et al., 2020). Cystamine (SS) is a GSH-sensitive linker that could offer response on the reduction environment such as tumor site, examples include the SS was used to prepare a GSH-responsive prodrug for photodiagnosis and photodynamic therapy of tumors (Li et al., 2019).

Prostate-specific membrane antigen (PSMA) is overexpressed on the surface of PCa cells (Afsharzadeh et al., 2020). Therefore, PSMA has been extensively used as a target antigen for targeted drug delivery in the treatment of PCa (Cohen et al., 2021). In the present study, to enhance the cancer cell-specific targeting, uptake, and retention (Nagesh et al., 2016), we design a PSMA-targeted, GSH-sensitive, polyethylene glycol (PEG)-contained drug delivery system to co-delivery DTX and EZL. First, PEG was conjugated with OA using a GSH-sensitive ligand: cystamine to achieve PEG-SS-OA. Then a targeting ligand—Glutamate-Urea-Lysine (GUL)—which could specifically bind to the PSMA was conjugated to PEG to achieve GUL-PEG-SS-OA (Cohen et al., 2021).

In this research, GUL modified, DTX and EZL co-loaded, GSH-sensitive nanoparticles (GUL-SS DTX/EZL-NPs) were prepared and evaluated *in vitro* and *in vivo* on human PCa cell lines and PCa cells bearing mice.

Materials and methods

Materials

DTX, EZL, 1-ethyl-3-(3-dimethylaminopropyl) carbodiimide (EDC), *N*-hydroxysuccinimide (NHS), dimethylaminopyridine (DMAP), and dimethyl sulfoxide (DMSO) were purchased from Sigma-Aldrich Co., Ltd. (St Louis, MO). Soybean lecithin (SL), OA, $HOOC\text{-}PEG_{2000}\text{-}COOH$ (PEG), and 1,2-dioleoyl-3-trimethylammonium-propane (DOTAP) were obtained from Avanti Polar Lipids (Alabaster, AL). Glu-Urea-Lys (GUL) with protecting groups of *tert*-butyl esters was purchased from ABX advanced biochemical compounds (Radeberg, Germany).

The human PCa cell lines (PC3 cells) were received from American Type Culture Collection (ATCC, Manassas, VA, USA).

BALB/c mice (20 ± 2 g) were purchased from Jiangsu ALF Biotechnology Co., Ltd. (Nanjing, China) and the animal experiments are operated in accordance with the National Institutes of Health Guide for the Care and Use of Laboratory Animals and approved by the Ethics Committee of the Affiliated Hospital of Jiangnan University (No. 2020121901).

Synthesis of GUL-PEG-SS-OA

PEG-SS-OA was synthesized by conjugating the amine groups of cystamine with the carboxyl groups of PEG and OA (Figure 1) (Tan & Wang, 2017). OA (1 equiv.), EDC (1.2 equiv.), and NHS (1.2 equiv.) were added in DMSO (10 mL) and stirred for 1 h (mixture 1). Cystamine (1 equiv.) was dissolved in DMSO (10 mL) and added dropwise to mixture 1, stirred for 10 h to achieve cystamine-OA. PEG (1.5 equivalents) was added dropwise to cystamine-OA, stirred for 10 h and dialyzed against excess ultrapure water for 24 h to get PEG-SS-OA. GUL-PEG-SS-OA was synthesized by covalent coupling of PEG-SS-OA with the amine group in the side chain of lysine in the GUL (Figure 1). Briefly, PEG-SS-OA (1 equiv.), GUL (1 equiv.), EDC (1.2 equiv.), and DMAP (0.1 equiv.) were dissolved in DMSO (10 mL), stirred for 10 h and dialyzed against excess ultrapure water for 24 h to get GUL-PEG-SS-OA. The formation of GUL-PEG-SS-OA was determined by using hydrogen-1 nuclear magnetic resonance (^{1}H NMR) and Fourier transform infrared spectroscopy (FTIR) analysis.

Preparation of GUL-SS DTX/EZL-NPs

GUL-SS DTX/EZL-NPs were prepared using a solvent diffusion and sonication method (Figure 2) (Pang et al., 2020). GUL-PEG-SS-OA (100 mg) and DOTAP (1%, wt/vol) were dispersed in ultrapure water (30 mL) and warmed to about 60 °C to prepare the aqueous phase. DTX (25 mg), EZL (25 mg), and SL (100 mg) was dissolved in acetone (20 mL) to get the lipid phase. The lipid phase was added dropwise into the aqueous

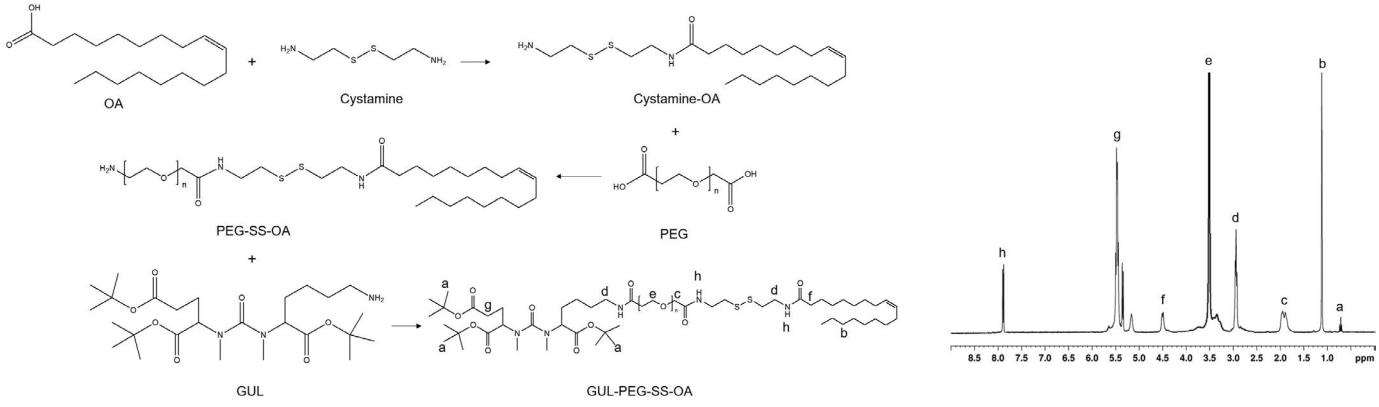

Figure 1. GUL-PEG-SS-OA was synthesized by conjugating PEG, OA with GUL. The formation of PEG-SS-OA was determined by using hydrogen-1 nuclear magnetic resonance (^{1}H NMR) analysis (1–8 in the ^{1}H NMR are marked one by one on the structure of GUL-PEG-SS-OA).

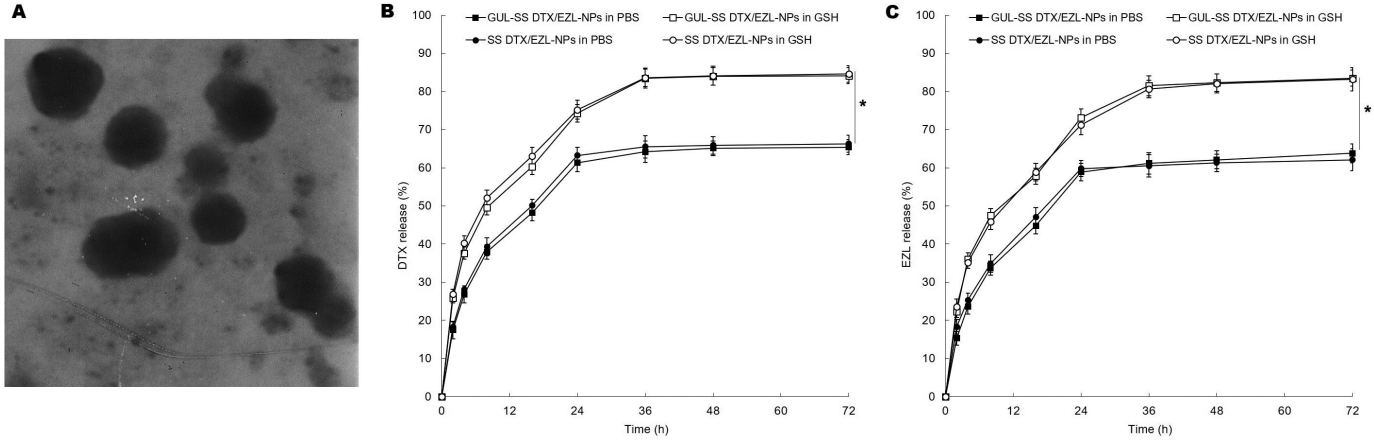

Figure 2. TEM image of GUL-SS DTX/EZL-NPs (A); *In vitro* drug release of DTX (B) and EZL (C) from GUL-SS DTX/EZL-NPs were evaluated in phosphate buffer solution (PBS) with or without GSH (10 mM) by a dialysis method. Results are presented as means ± SD. *$p < .05$.

phase, sonicated for 10 min, and then stirred for 10 h to evaporate the organic solvent. GUL-SS DTX/EZL-NPs were purified by washing three times using an Amicon Ultra-4 centrifuge filter (molecular weight cutoff of 30 kDa).

Blank NPs without drugs (GUL-SS NPs) were prepared using no drugs in the lipid phase.

Single drug-loaded NPs (SS DTX-NPs and SS EZL-NPs) were prepared using DTX or EZL only in the lipid phase.

Characterization of GUL-SS DTX/EZL-NPs

The mean particle size, size distribution (polydispersity, PDI), and zeta potential of the GUL-SS DTX/EZL-NPs and other NPs were determined by dynamic light scattering (DLS) using a NanoZS Zetasizer (Malvern Instruments Ltd., Malvern, UK) (Wang et al., 2020). A transmission electron microscope (JEOL, Tokyo, Japan) was used to record the surface morphology of DTX/EZL-NPs. DTX content was analyzed through high-performance liquid chromatography (HPLC) (Guan et al., 2016). EZL content was analyzed at 254 nm via a UV system (Jiang et al., 2020). The formulas for drug loading content (DL) and entrapment efficiency (EE) are:

$$\mathrm{DL}\ (\%) = \text{Drugs entrapped in NPs / Total weight of NPs} \times 100;$$

$$\mathrm{EE}\ (\%) = \text{Drugs entrapped in NPs / Total weight of drugs} \times 100.$$

The stability of nanoparticles was tested at physiological temperature and pH. NPs were kept undisturbed at 37 °C in various concentrations of bicarbonate buffer, 0.1 M, 0.01 M, and 0.001 M, pH 7.4. Accumulation of NPs at the bottom of microcentrifuge tube was used as a sign of agglomerate formation (Sonkusre et al., 2014).

In vitro drug release

In vitro drug release from GUL-SS DTX/EZL-NPs was evaluated in phosphate buffer solution (PBS) with or without GSH (10 mM) by a dialysis method (Conte et al., 2018). GUL-SS DTX/EZL-NPs was dispersed in PBS and placed in a dialysis bag (molecular weight cutoff of 3500 Da). The sample was placed in PBS under shaken (100 rpm) at 37 °C. The release medium (1 mL) was taken out at determined time points and replaced with an equal volume of fresh medium. The amount of drugs released was determined by the methods in the above section.

Cellular uptake

PC3 cells were seeded on 96-well plates (1×10^4 cells per well). Coumarin 6-loaded NPs (C6-loaded NPs) were prepared the same way as 'Preparation of GUL-SS DTX/EZL-NPs' by adding Coumarin 6 (10 mg) into the lipid phase (Hong et al., 2019). Various kinds of C6-loaded NPs (100 µL) were added to each well and incubated for 4 h. Then the cells were washed with PBS and were detached with trypsin/EDTA. The cells were re-suspended in PBS, photographed by fluorescence microscopy, and analyzed using a flow cytometer (BD Biosciences, San Jose, CA).

In vitro cell viability

The cytotoxicity of NPs was determined by 3-(4,5-dim ethylthiazol-2-yl)-2,5-diphenyltetrazolium bromide (MTT) assay (Li et al., 2017). PC3 cells were seeded on 96-well plates (1×10^4 cells per well) and then exposed to free drugs and NPs at various concentrations for 72 h, viability was determined by the MTT assay. The formula for relative cell viability is: (The absorbance of the sample well)/(The absorbance of the control well) × 100.

In vivo tissue distribution and tumor inhibition effect

BALB/c mice were injected with PC3 cells (10^5 cells in 100 µL of PBS) into the right flank to obtain tumor-bearing xenograft (Juang et al., 2019). When tumor volume reached about 100 mm^3, the mice (10 each group) were injected with GUL-SS DTX/EZL-NPs, GUL-SS NPs, SS DTX-NPs, SS EZL-NPs, free DTX/EZL, and 0.9% saline every three days from day 0 to day 18. Tissue distribution of drugs was determined after 1 h and 48 h

of the first injection. Tissues were excised and homogenized in lysis buffer, mixed with methanol, and then centrifuged for 30 min. Drug quantitative analysis was performed as described in 'Characterization of GUL-SS DTX/EZL-NPs' section. The tumor volume and body weight changes were tested every 3 days after injection. The formula for tumor volume is: the longest axis × the perpendicular shorter tumor axis^2 × 0.5.

Statistical analysis

The significance of differences was assessed using two-tailed Student's *t* tests. Results are presented as means ± SD. Differences were considered to be significant at a level of $p < .05$ (*).

Results

Characterization of GUL-PEG-SS-OA and GUL-SS DTX/EZL-NPs

The ^{1}H NMR spectrum of GUL-PEG-SS-OA was presented in Figure 1 with the proton signals marked corresponded to the structural formula. The peaks c, d, f, and h confirmed the formation of the amido linkage. FTIR ν/cm^{-1}: 3439 (–NH–); 2931(–CH_2–, –CH–); 1659(–HN–CO–, –HN–); 1422(–CH_2CO–).

The particle size, PDI, zeta potential, DL, and EE of the GUL-SS DTX/EZL-NPs and other NPs are summarized in Table 1. GUL-SS DTX/EZL-NPs was uniform particles (Figure 2A), showing a size of 143.7 ± 4.1 nm, with a PDI of 0.162 ± 0.037 and a zeta potential of +29.1 ± 2.4 mV. The DTX and EZL EE of NPs was around 90%. There is no accumulation of NPs at the bottom of microcentrifuge tube, which could prove the stability of NPs.

In vitro drug release

The drug release behaviors of NPs were evaluated in the medium with or without GSH. Figure 2 illustrates that although NPs showed sustained release behaviors both in PBS and GSH solution, DTX and EZL released faster and more sufficient from NPs in the presence of GSH ($p < .05$). Over 80% of drugs were released from NPs after 36 h of study in the GSH containing medium, which was higher than the about 60% of total release in PBS. GUL-SS DTX/EZL-NPs and SS DTX/EZL-NPs exhibited similar release behaviors.

Cellular uptake

The cellular uptake results of NPs are displayed in Figure 3. The fluorescence images and flow cytometry results showed that more C6-loaded GUL-SS DTX/EZL-NPs (70.3%) were taken by the cells compared with SS DTX/EZL-NPs, SS DTX-NPs, and SS EZL-NPs, indicating the improved cell entry ability of the modified NPs.

In vitro cell viability

In vitro cell viability of NPs was evaluated to determine the cytotoxicity of the systems. Figure 4 illustrates blank NPs did not cause all the cytotoxicity. Drugs containing formulations showed obvious cytotoxicity compared with the saline control group ($p < .05$). Dual drugs loaded, modified GUL-SS DTX/EZL-NPs exhibited higher cell inhibition efficiency than single drug loaded NPs and free DTX/EZL ($p < .05$).

In vivo tissue distribution and tumor inhibition effect

In vivo tissue distribution of drugs is presented in Figure 5. At 48 h post injection, the drugs accumulation in the tumor of NPs were higher than that of free drugs ($p < .05$), in the meantime, GUL-SS DTX/EZL-NPs showed higher tumor distribution than that of SS DTX-NPs and SS EZL-NPs ($p < .05$). More free drugs were distributed in the kidney compared with the NPs formulas ($p < .05$). Figure 6A illustrates the *in vivo* tumor inhibition effect of GUL-SS DTX/EZL-NPs, which was significantly higher than SS DTX-NPs and free DTX/EZL ($p < .05$). Blank GUL-SS NPs did not exhibit effects on tumor bearing mice, which showed a similar effect with 0.9% saline control groups. The body weight of free drugs groups decreased along with the time, while NPs groups did not cause body weight loss (Figure 6B).

Discussion

The present study aimed to develop a GUL-modified, GSH-sensitive ligand, and used for the construction of nanoparticles. First, GUL-PEG-SS-OA was synthesized. OA is a lipid that was widely applied for preparation of nano-systems. PEG-modification was reported as the most noteworthy modification to prevent interactions with plasma proteins, thus retarding recognition and removal by the reticular endothelial system (RES) (Gunaseelan et al., 2010). In this study, GUL-PEG-SS-OA was synthesized and used for NPs preparation.

GUL-SS DTX/EZL-NPs were prepared using a solvent diffusion and sonication method. DOTAP is a double-tailed cationic lipid which is used as the surfactant of nanoparticles, and showed less toxicity than the single-tailed cationic lipid such as cetyltrimethylammonium bromide (CTAB). The zeta potential of NPs was positive due to the use of cationic DOTAP. Particle sizes smaller than 200 nm are conducive to

Table 1. The particle size, PDI, zeta potential, DL, and EE of NPs.

				DL (%)		EE (%)	
NPs	Diameter (nm)	PDI	Zeta potential (mV)	DTX	EZL	DTX	EZL
GUL-SS DTX/EZL-NPs	143.7 ± 4.1	0.162 ± 0.037	+ 29.1 ± 2.4	6.3 ± 0.7	6.1 ± 0.6	90.9 ± 2.7	89.5 ± 2.9
GUL-SS NPs	141.6 ± 3.8	0.145 ± 0.022	+ 27.9 ± 2.7	/	/	/	/
SS DTX-NPs	121.9 ± 3.7	0.169 ± 0.029	+ 19.1 ± 2.1	9.1 ± 0.7	/	90.3 ± 3.3	/
SS EZL-NPs	118.6 ± 4.1	0.178 ± 0.031	+ 20.2 ± 1.8	/	7.5 ± 1.1	/	88.3 ± 2.6

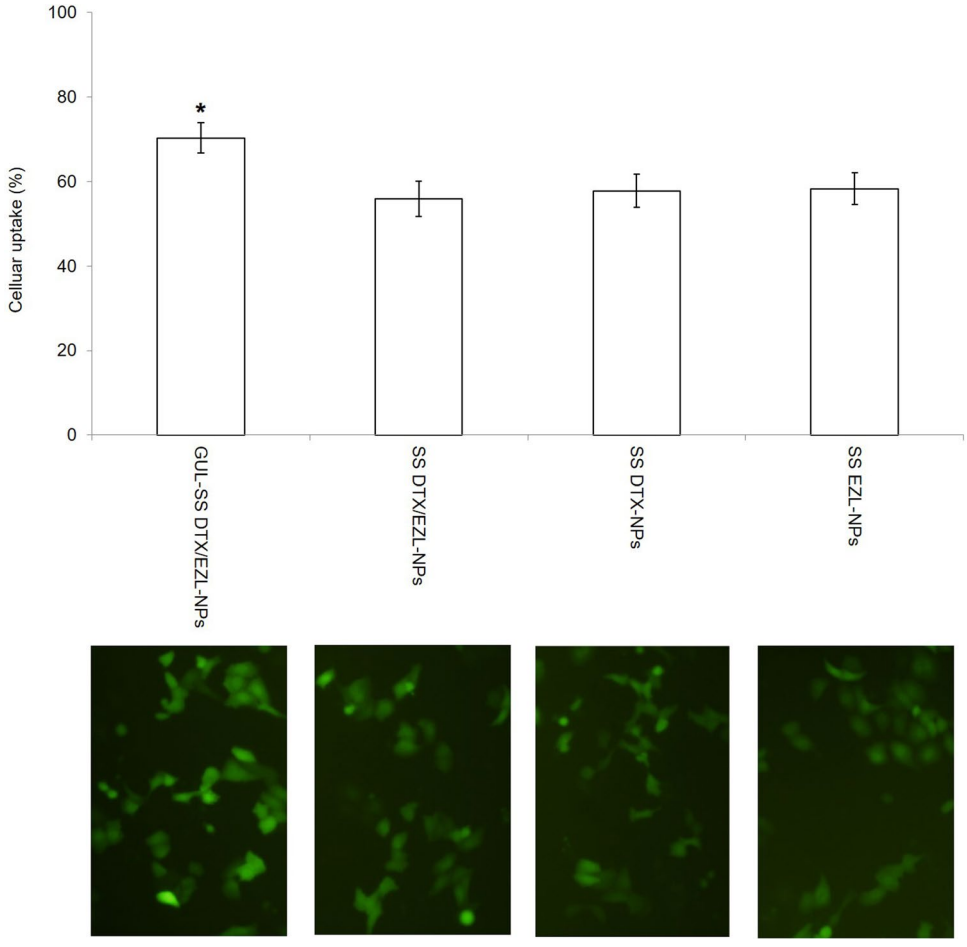

Figure 3. The cellular uptake efficiency of C6-loaded NPs. *$p < .05$.

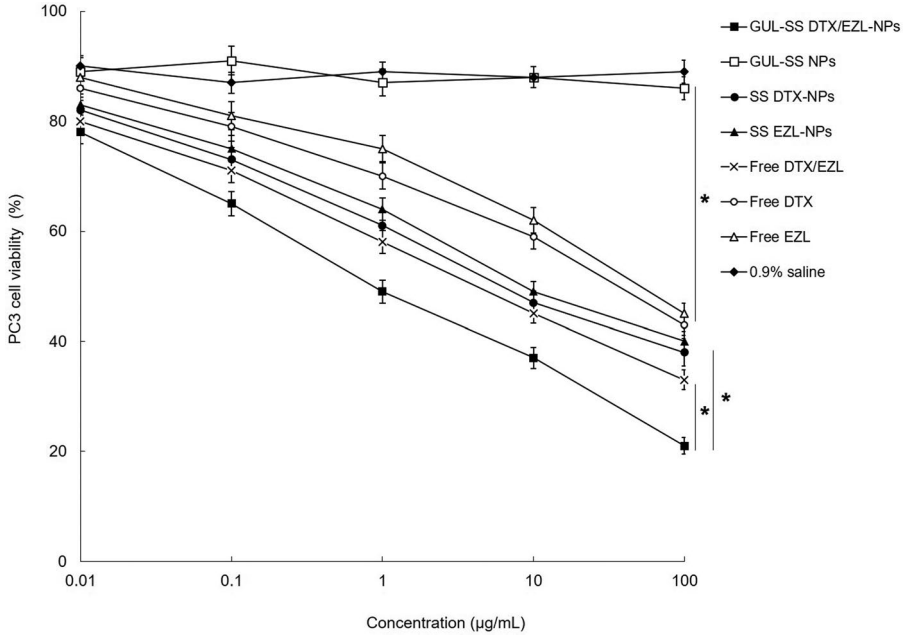

Figure 4. The cytotoxicity of NPs was determined by MTT assay. Results are presented as means ± SD. *$p < .05$.

drug accumulation at the tumor site based on the EPR effect, thereby reducing the drug dose and minimizing toxicity (Wang et al., 2020). High drug encapsulation efficacy is required for the construction of a successful nanoparticle system. GUL-SS DTX/EZL-NPs in this research showed a size of 143.7 ± 4.1 nm, with an EE around 90%.

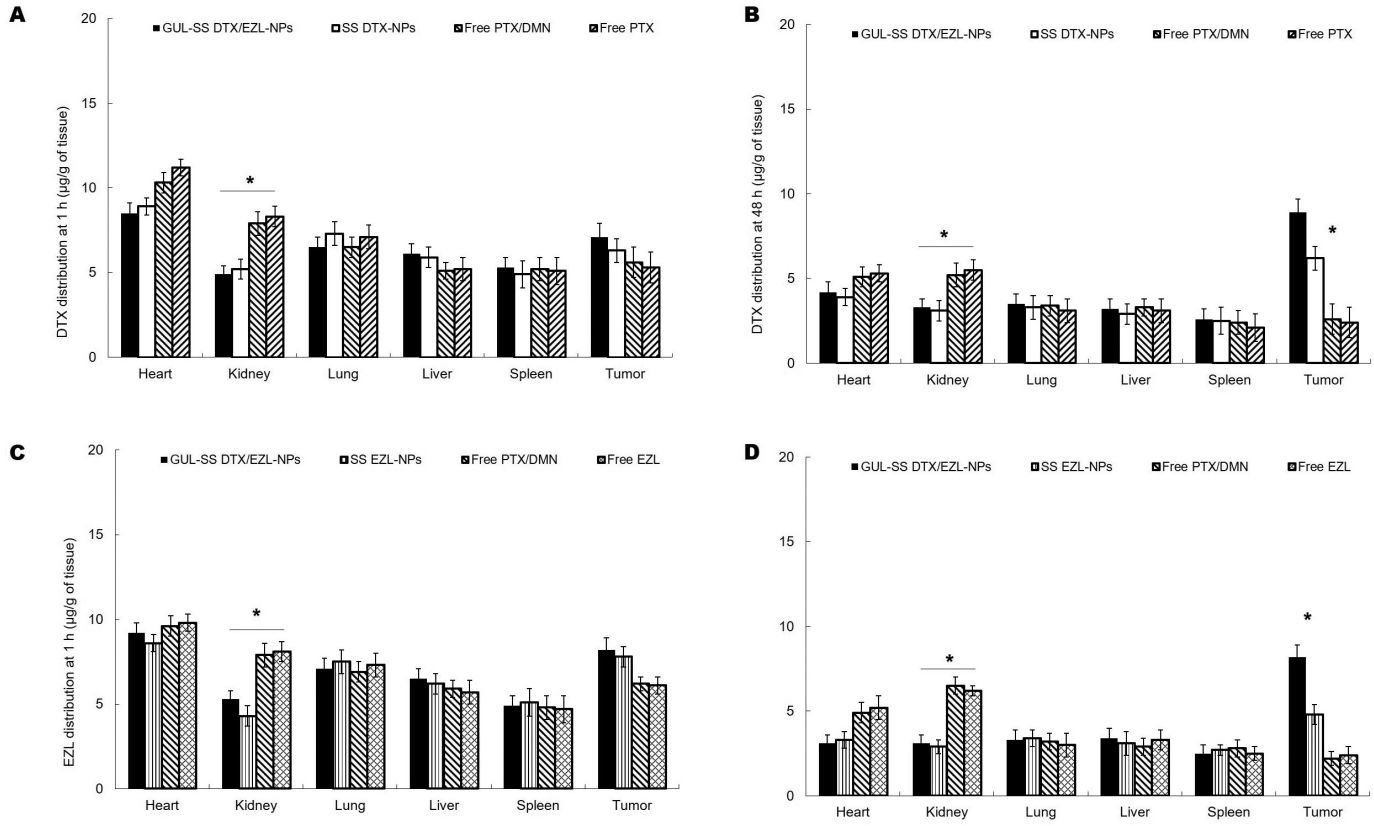

Figure 5. *In vivo* tissue distribution of DTX after 1 h (A) and 48 h (B) of administration; tissue distribution of EZL after 1 h (C) and 48 h (D) of administration. Results are presented as means ± SD. *$p < .05$.

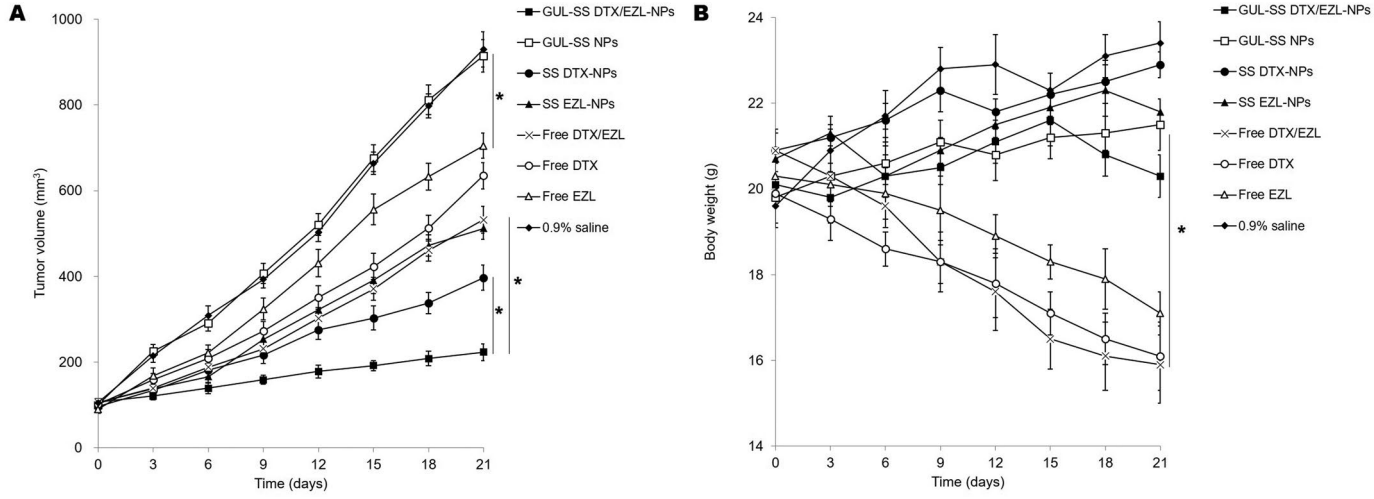

Figure 6. *In vivo* tumor inhibition effect (A) and body weight changes (B). Results are presented as means ± SD. *$p < .05$.

To further evaluate the GSH-sensitive drug release of NPs, GUL-SS DTX/EZL-NPs were tested in PBS with or without GSH by a dialysis method. DTX and EZL released faster and more sufficient from NPs in the presence of GSH, indicating GSH-sensitive drug release (Huang et al., 2019). GUL-SS DTX/EZL-NPs exhibited similar release behavior as unmodified SS DTX/EZL-NPs, which excluded the influence of the GUL surface modification on the drug release.

The NPs also showed high tumor cell uptake efficiency, which is in accordance with the results of Liu et al. (2018). They argued that the results of qualitative and quantitative studies of cellular uptake indicate that the functionalization of NPs encapsulation played a key role in the uptake of drugs in cancer cells. *In vitro* cell viability of NPs illustrated that blank NPs did not cause all the cytotoxicity, which may be the proof of the low toxicity of the materials used in the preparation (Wu et al., 2020). GUL-SS DTX/EZL-NPs exhibited higher cell inhibition efficiency than single drug loaded NPs, which could be explained by the synergistic effect of the dual drugs co-loaded in one system and the PSMA targeted GUL

that delivered more drugs to the cells (Nan, 2019). Drug-loaded NPs showed improved cytotoxicity compared with free drugs, which proved to be good potential systems for anticancer applications (Al-Dulimi et al., 2020; Mirhadi et al., 2020).

In vivo drugs distribution of NPs, when compared with their free drugs counterparts, higher in the tumor tissue and lower in the kidney, could decrease the side effects during the tumor therapy (Duan & Liu, 2018). The nanocarrier faces several challenges while in the circulation, including maintaining adequate bioavailabilty and avoiding clearance by the kidney (El-Sayed et al., 2009). In this study, drug-loaded NPs showed higher distribution in the tumor and lower accumulation in the kidney than free DTX/EZL, indicating the less toxicity of the NPs system *in vivo*. GUL-SS DTX/EZL-NPs showed higher tumor distribution than unmodified SS DTX-NPs and SS EZL-NPs, which could be the evidence of the surface modification (Yu et al., 2010). Differences in body weight were insignificant between the drug-loaded NPs-treated mice and control mice, which were in line with the distribution experiments that could be the evidence of the safety of the nanosystem constructed in the present research (Huang et al., 2019; Sulaiman et al., 2020). *In vivo* tumor inhibition effect of GUL-SS DTX/EZL-NPs was significantly higher than single drug containing NPs and free DTX/EZL, which was concluded by Hong et al that the dual drugs encapsulated NPs had an effective biological function than the single drug-loaded ones *in vivo* (Pang et al., 2020). GUL-SS DTX/EZL-NPs showed better tumor inhibition ability than free DTX/EZL, which was explained by Zhu et al. that the lipid NPs could exhibit high biocompatibility and bioavailability due to its similar character with the cell membranes (Zhu et al., 2017).

Conclusion

In the present research, GUL-SS DTX/EZL-NPs showed high cancer cell uptake of about 70%, as well as higher cell inhibition efficiency than single drug-loaded specific NPs and free drugs. GUL-SS DTX/EZL-NPs showed the most prominent tumor inhibition ability and less systemic toxicity. These results illustrated that GUL-SS DTX/EZL-NPs could be used as a promising system for PCa therapy. However, the expanded reproduction of the NPs and the use of this system from the bench to bedside should be further considered.

Disclosure statement

The authors report no conflict of interest.

Funding

The author(s) reported there is no funding associated with the work featured in this article.

References

A safety and efficacy study of oral MDV3100 in chemotherapy-naïve patients with progressive metastatic prostate cancer (PREVAIL) (NCT01212991). (2014) Available at: http://clinicaltrials.gov/ct2/show/NCT01212991 [last accessed 9 Feb 2014].

Afsharzadeh M, Hashemi M, Babaei M, et al. (2020). PEG-PLA nanoparticles decorated with small-molecule PSMA ligand for targeted delivery of galbanic acid and docetaxel to prostate cancer cells. J Cell Physiol 235:4618–30.

Al-Dulimi A, Al-Saffar A, Sulaiman G, et al. (2020). Immobilization of l-asparaginase on gold nanoparticles for novel drug delivery approach as anti-cancer agent against human breast carcinoma cells. J Mater Res Technol 9:15394–411.

Argenziano M, Lombardi C, Ferrara B, et al. (2018). Glutathione/pH-responsive nanosponges enhance strigolactone delivery to prostate cancer cells. Oncotarget 9:35813–29.

Berthold DR, Pond GR, Soban F, et al. (2008) Docetaxel plus prednisone or mitoxantrone plus prednisone for advanced prostate cancer: updated survival in the TAX 327 study. J Clin Oncol 26:242–5.

Cohen L, Assaraf YG, Livney YD. (2021). Novel selectively targeted multifunctional nanostructured lipid carriers for prostate cancer treatment. Pharmaceutics 14:88.

Conte C, Mastrotto F, Taresco V, et al. (2018). Enhanced uptake in 2D- and 3D- lung cancer cell models of redox responsive PEGylated nanoparticles with sensitivity to reducing extra- and intracellular environments. J Control Release. 277:126–41.

Duan W, Liu Y. (2018). Targeted and synergistic therapy for hepatocellular carcinoma: monosaccharide modified lipid nanoparticles for the co-delivery of doxorubicin and sorafenib. Drug Des Devel Ther 12:2149–61.

El-Sayed A, Futaki S, Harashima H. (2009). Delivery of macromolecules using arginine-rich cell-penetrating peptides: ways to overcome endosomal entrapment. 11:13–22.

Fizazi K, Scher HI, Miller K, et al. (2014). Effect of enzalutamide on time to first skeletal-related event, pain, and quality of life in men with castration-resistant prostate cancer: results from the randomised, phase 3 AFFIRM trial. Lancet Oncol 15:1147–56.

Guan Q, Sun D, Zhang G, et al. (2016). Docetaxel-loaded self-assembly stearic acid-modified *Bletilla striata* polysaccharide micelles and their anticancer effect: preparation, characterization, cellular uptake and in vitro evaluation. Molecules 21:1641.

Gunaseelan S, Gunaseelan K, Deshmukh M, et al. (2010). Surface modifications of nanocarriers for effective intracellular delivery of anti-HIV drugs. Adv Drug Deliv Rev 62:518–31.

Hong Y, Che S, Hui B, et al. (2019). Lung cancer therapy using doxorubicin and curcumin combination: Targeted prodrug based, pH sensitive nanomedicine. Biomed Pharmacother 112:108614.

Huang H, Dong Y, Zhang Y, et al. (2019). GSH-sensitive Pt(IV) prodrug-loaded phase-transitional nanoparticles with a hybrid lipid-polymer shell for precise theranostics against ovarian cancer. Theranostics 9:1047–65.

Jabir M, Sahib UI, Taqi Z, et al. (2020). Linalool-loaded glutathione-modified gold nanoparticles conjugated with CALNN peptide as apoptosis inducer and NF-κB translocation inhibitor in SKOV-3 cell line. Int J Nanomedicine 15:9025–47.

Jemal A, Bray F, Center MM. (2011). Global cancer statistics. CA Cancer J Clin 61:69–90.

Jiang W, Chen J, Gong C, et al. (2020). Intravenous delivery of enzalutamide based on high drug loading multifunctional graphene oxide nanoparticles for castration-resistant prostate cancer therapy. J Nanobiotechnology 18:50.

Juang V, Chang CH, Wang CS, et al. (2019). pH-responsive PEG-shedding and targeting peptide-modified nanoparticles for dual-delivery of irinotecan and microRNA to enhance tumor-specific therapy. Small 15:e1903296.

Kellokumpu-Lehtinen PL, Harmenberg U, Joensuu T, et al. (2013). PROSTY study group. 2-Weekly versus 3-weekly docetaxel to treat castration-resistant advanced prostate cancer: a randomised, phase 3 trial. Lancet Oncol. 14:117–24.

Kim D, Park C, Meghani NM, et al. (2020). Utilization of a fattigation platform gelatin-oleic acid sodium salt conjugate as a novel solubilizing adjuvant for poorly water-soluble drugs via self-assembly and nanonization. Int J Pharm 575:118892.

Li F, Mei H, Gao Y, et al. (2017). Co-delivery of oxygen and erlotinib by aptamer-modified liposomal complexes to reverse hypoxia-induced drug resistance in lung cancer. Biomaterials 145:56–71.

Li J, Djenaba JA, Soman A, et al. (2012). Recent trends in prostate cancer incidence by age, cancer stage, and grade, the United States, 2001-2007. Prostate Cancer 2012:691380.

Li K, Dong W, Qiu L, et al. (2019). A new GSH-responsive prodrug of 5-aminolevulinic acid for photodiagnosis and photodynamic therapy of tumors. Eur J Med Chem 181:111582.

Liu J, Cheng H, Han L, et al. (2018). Synergistic combination therapy of lung cancer using paclitaxel- and triptolide-coloaded lipid-polymer hybrid nanoparticles. Drug Des Devel Ther 12:3199–209.

Marín-Aguilera M, Reig Ò, Milà-Guasch M, et al. (2019). The influence of treatment sequence in the prognostic value of TMPRSS2-ERG as biomarker of taxane resistance in castration-resistant prostate cancer. Int J Cancer 145:1970–81.

Mirhadi E, Mashreghi M, Faal Maleki M, et al. (2020) Redox-sensitive nanoscale drug delivery systems for cancer treatment. Int J Pharm 589:119882.

Nagesh PKB, Johnson NR, Boya VKN, et al. (2016). PSMA targeted docetaxel-loaded superparamagnetic iron oxide nanoparticles for prostate cancer. Colloids Surf B Biointerfaces 144:8–20.

Nan Y. (2019). Lung carcinoma therapy using epidermal growth factor receptor-targeted lipid polymeric nanoparticles co-loaded with cisplatin and doxorubicin. Oncol Rep 42:2087–96.

Pang J, Xing H, Sun Y, et al. (2020). Non-small cell lung cancer combination therapy: hyaluronic acid modified, epidermal growth factor receptor targeted, pH sensitive lipid-polymer hybrid nanoparticles for the delivery of erlotinib plus bevacizumab. Biomed Pharmacother 125:109861.

Phan UT, Nguyen KT, Vo TV, Duan W, et al. (2016). Investigation of fucoidan-oleic acid conjugate for delivery of curcumin and paclitaxel. Anticancer Agents Med Chem 16:1281–7.

Scher HI, Fizazi K, Saad F, et al. (2012). AFFIRM Investigators. Increased survival with enzalutamide in prostate cancer after chemotherapy. N Engl J Med 367:1187–97.

Sonkusre P, Nanduri R, Gupta P, Cameotra SS. (2014). Improved extraction of intracellular biogenic selenium nanoparticles and their specificity for cancer chemoprevention. J Nanomed Nanotechnol 05:194.

Sulaiman GM, Waheeb HM, Jabir MS, et al. (2020). Hesperidin loaded on gold nanoparticles as a drug delivery system for a successful biocompatible, anti-cancer, anti-inflammatory and phagocytosis inducer model. Sci Rep. Jun 910:9362.

Tan S, Wang G. (2017). Redox-responsive and pH-sensitive nanoparticles enhanced stability and anticancer ability of erlotinib to treat lung cancer in vivo. Drug Des Devel Ther 11:3519–29.

Tannock IF, de Wit R, Berry WR, et al. (2004). TAX 327 Investigators. Docetaxel plus prednisone or mitoxantrone plus prednisone for advanced prostate cancer. N Engl J Med 351:1502–12.

Wang J, Su G, Yin X, et al. (2019) Non-small cell lung cancer-targeted, redox-sensitive lipid-polymer hybrid nanoparticles for the delivery of a second-generation irreversible epidermal growth factor inhibitor-Afatinib: in vitro and in vivo evaluation. Biomed Pharmacother 120:109493.

Wang Z, Zang A, Wei Y, et al. (2020). Hyaluronic acid capped, irinotecan and gene co-loaded lipid-polymer hybrid nanocarrier-based combination therapy platform for colorectal cancer. Drug Des Devel Ther 14:1095–105.

Wu R, Zhang Z, Wang B, et al. (2020). Combination chemotherapy of lung cancer – co-delivery of docetaxel prodrug and cisplatin using aptamer-decorated lipid-polymer hybrid nanoparticles. Drug Des Devel Ther 14:2249–61.

Xu C, Song RJ, Lu P, et al. (2018). pH-triggered charge-reversal and redox-sensitive drug-release polymer micelles codeliver doxorubicin and triptolide for prostate tumor therapy. Int J Nanomedicine 13:7229–49.

Xu Z, Liu S, Kang Y, Wang M. (2015). Glutathione- and pH-responsive nonporous silica prodrug nanoparticles for controlled release and cancer therapy. Nanoscale 7:5859–68.

Yan J, Wang Y, Zhang X, et al. (2016). Targeted nanomedicine for prostate cancer therapy: docetaxel and curcumin co-encapsulated lipid-polymer hybrid nanoparticles for the enhanced anti-tumor activity in vitro and in vivo. Drug Deliv 23:1757–62.

Yu W, Liu C, Liu Y, et al. (2010). Mannan-modified solid lipid nanoparticles for targeted gene delivery to alveolar macrophages. Pharm Res 27:1584–96. Epub 2010 Apr 27. PMID: 20422265.

Zhang T, Ma J, Li C, et al. (2017). Core–shell lipid polymer nanoparticles for combined chemo and gene therapy of childhood head and neck cancers. Oncol Rep 37:1653–61.

Zhu B, Yu L, Yue Q. (2017). Co-delivery of vincristine and quercetin by nanocarriers for lymphoma combination chemotherapy. Biomed Pharmacother 91:287–94.